Journal of Cerebral Blood Flow & Metabolism (2015) 35, 2021–2031

www.jcbfm.com

ORIGINAL ARTICLE

Recombinant tissue-type plasminogen activator transiently enhances blood–brain barrier permeability during cerebral ischemia through vascular endothelial growth factor-mediated endothelial endocytosis in mice

Yasuhiro Suzuki[1,2], Nobuo Nagai[3], Kasumi Yamakawa[2], Yoshinori Muranaka[4], Kazuya Hokamura[2] and Kazuo Umemura[2]

Recombinant tissue-type plasminogen activator (rt-PA) modulates cerebrovascular permeability and exacerbates brain injury in ischemic stroke, but its mechanisms remain unclear. We studied the involvement of vascular endothelial growth factor (VEGF)-mediated endocytosis in the increase of blood–brain barrier (BBB) permeability potentiated by rt-PA after ischemic stroke. The rt-PA treatment at 4 hours after middle cerebral artery occlusion induced a transient increase in BBB permeability after ischemic stroke in mice, which was suppressed by antagonists of either low-density lipoprotein receptor families (LDLRs) or VEGF receptor-2 (VEGFR-2). In immortalized bEnd.3 endothelial cells, rt-PA treatment upregulated VEGF expression and VEGFR-2 phosphorylation under ischemic conditions in an LDLR-dependent manner. In addition, rt-PA treatment increased endocytosis and transcellular transport in bEnd.3 monolayers under ischemic conditions, which were suppressed by the inhibition of LDLRs, VEGF, or VEGFR-2. The rt-PA treatment also increased the endocytosis of endothelial cells in the ischemic brain region after stroke in mice. These findings indicate that rt-PA increased BBB permeability via induction of VEGF, which at least partially mediates subsequent increase in endothelial endocytosis. Therefore, inhibition of VEGF induction may have beneficial effects after thrombolytic therapy with rt-PA treatment after stroke.

Journal of Cerebral Blood Flow & Metabolism (2015) **35,** 2021–2031; doi:10.1038/jcbfm.2015.167; published online 29 July 2015

Keywords: brain ischemia; endothelial endocytosis; tissue-type plasminogen activator; vascular endothelial growth factor; vascular permeability

INTRODUCTION

Recombinant tissue-type plasminogen activator (rt-PA), a serine proteinase, is thought to exacerbate ischemic brain damage by direct neurotoxicity[1–3] and by increasing the permeability of the blood–brain barrier (BBB) in ischemic regions.[4–9] This increase occurs via activation of low-density lipoprotein receptor-related protein (LRP).[4–9] Lipoprotein receptor-related protein is a member of the LDL receptor family (LDLRs), which has important roles in the removal of lipoproteins and biologically diverse ligands in the liver for the scavenging and recycling of various proteases.[10,11] Lipoprotein receptor-related protein is also known as a major binding site of rt-PA.[11] As LRP was selectively upregulated in endothelial cells under ischemic stress,[4] rt-PA may increase BBB permeability via LRP activation.

Although the deleterious effect of rt-PA after ischemic stroke has been widely accepted, it remains unclear whether blood-derived rt-PA penetrates the brain and contributes to these detrimental processes in the cerebral parenchyma. Intravenously administered rt-PA was shown to cross brain endothelial cells via transcytosis without compromising BBB integrity,[5,12] whereas rt-PA was also found to enter the parenchyma under pathologic conditions, where it further enhances BBB breakdown.[6]

The BBB is formed by interendothelial tight junctions between endothelial cells together with pericytes, astrocytes, and basement membrane in the vasculature. Furthermore, as cerebrovascular function is regulated by the neuronal environment, these components, the BBB and neurons, are thought to form a functional unit called the neurovascular unit. The BBB permeability is regulated in response to various stimulators or stressors, which can exert beneficial or deleterious effects on the brain depending on the context, timing, and functional cellular outcomes of signaling.[13] The BBB permeability can increase via two processes: loosening the tight junctions between endothelial cells for increased paracellular transport and activation of endocytosis at the luminal surface of endothelial cells for increased transcellular transport. Vascular endothelial growth factor (VEGF or VEGF-A), a molecular stimulator that binds to two receptor-coupled protein tyrosine kinases, VEGF receptor 1 (VEGFR-1, Flt-1) and 2 (VEGFR-2, KDR), regulates the dissociation of endothelial cell junctions[14] and endocytosis[15] and subsequent increase in vessel permeability,

[1]School of Pharmaceutical Sciences, Ohu University, Koriyama, Japan; [2]Department of Pharmacology, Hamamatsu University School of Medicine, Hamamatsu, Japan; [3]Department of Animal Bioscience, Faculty of Bioscience, Nagahama Institute of Bio-Science and Technology, Nagahama, Japan and [4]Ultrastructure Laboratory, Research Equipment Center, Hamamatsu University School of Medicine, Hamamatsu, Japan. Correspondence: Dr Y Suzuki, School of Pharmaceutical Sciences, Ohu University, 31-1 Misumido, Tomita-machi, Koriyama, Fukushima 963-8611, Japan.
E-mail: ya-suzuki@pha.ohu-u.ac.jp
This study was supported by JSPS KAKENHI Grant-in-Aid for Young Scientists (B) Number 23790289 to YS.
Received 4 July 2014; revised 9 June 2015; accepted 11 June 2015; published online 29 July 2015

which causes vasogenic edema and contributes to cerebral swelling at the early stage after ischemic stroke.[16] The VEGF is induced in endothelial cells through accumulation of hypoxia-inducible factor-1*α* (HIF-1*α*),[17] a major regulator of transcriptional activation of hypoxia-related genes.[18,19]

Here, we investigated the effect of rt-PA treatment on BBB integrity with a focus on endothelial cells. We found that delayed rt-PA treatment induced a transient increase in BBB permeability through the activation of LRP and subsequent VEGF induction in a murine stroke model.[20] Furthermore, we evaluated the involvement of VEGF-mediated endocytosis and transcellular transport in the increase in BBB permeability *in vitro* using bEnd.3 brain-derived immortalized endothelial cells and *in vivo*.

MATERIALS AND METHODS

Experimental Design

Animals. Male C57Bl/6 mice (SLC, Hamamatsu, Japan) weighing 20 to 30 g (age, 3 months) were used. The animals were fed standard mouse chow and received water *ad libitum*, and a diurnal light cycle of 12 hours was maintained at 23 ± 2 °C. All animal experimental protocols and any relevant details regarding animal welfare and drug side effects were approved by the ethical committee of the Hamamatsu University School of Medicine. The ethical committee is based on the Ministry of the Environment Guidelines for the Care and Use of Animals in Research and Guidelines for Proper Conduct of Animal Experiments (2006). All the animal experiments were performed in accordance with the ARRIVE (Animal Research: Reporting *In Vivo* Experiments) guidelines.

Assessment of blood–brain barrier permeability in a mouse stroke model. Vascular permeability after middle cerebral artery (MCA) occlusion in mice was determined by Evans blue (EB, Sigma-Aldrich, St Louis, MO, USA) leakage. Focal cerebral ischemia was induced by permanent ligation of the MCA. Briefly, mice were anesthetized with 2% halothane in oxygen, and rectal temperature was maintained at 37 °C. The left temporal muscle was transected and the skull was exposed. A 1-mm opening was made at the region over the MCA on the skull. The meninges were removed, the MCA was occluded by ligation with a 10–0 nylon thread (Ethylon, Neuilly, France) and transected on the distal side, and the temporal muscle and skin were sutured back in place.[20]

At 4 hours after MCA occlusion, rt-PA (Alteplase; Activacin, Kyowa Hakko Kirin, Tokyo, Japan) or solvent (phosphate buffer containing with 0.66 mol/L L-arginine and 0.03% Tween 80) was administered intravenously as a bolus from the tail vein.[4] The EB extravasation was assessed after different durations of 10 mg/kg rt-PA or solvent treatment (6 ($n = 8$ per group), 9 ($n = 6$ per group), 12 ($n = 5$ per group), 24 ($n = 5$ for solvent or $n = 4$ for with rt-PA), or 72 hours ($n = 5$ per group)), all initiated at 4 hours after permanent MCA occlusion (Figure 1A). Seven mice were excluded after randomization because of failure to inject rt-PA or EB. Sham-operated mice subjected to rt-PA treatment were also studied (6, 9, 12, 24, or 72 hours ($n = 6$ per group), all initiated at 4 hours after permanent MCA occlusion (Figure 1A)). The experiments were performed in a masked manner.

To study the effect of the timing of rt-PA administration after MCA occlusion, rt-PA or solvent was intravenously administered 1, 4, 7, 22, or 70 hours after permanent MCA occlusion as a bolus from the tail vein. Animals were euthanized 2 hours after rt-PA treatment (Figure 1B).[4] The group sizes for each treatment condition were as follows: 1 hour, $n = 6$ in both the solvent and rt-PA groups; 4 hours, $n = 8$ per group; 7 hours, $n = 6$ per group; 22 hours, $n = 5$ per group; and 70 hours, $n = 5$ in the solvent group and $n = 6$ in the rt-PA group. Three mice were excluded after randomization because of failure to inject rt-PA or EB. To evaluate dose dependency, EB extravasation was additionally assessed after treatment with a dose of 0.9 or 3 mg/kg rt-PA ($n = 6$ per group) or solvent ($n = 2$ per group). All the treatments were administered at 4 hours after permanent MCA occlusion.

The involvement of LRP was studied by the intravenous administration of receptor-associated protein (RAP, 1 or 2 mg/kg; Progen, Heidelberg, Germany), a general antagonist of LDLRs, as a bolus 5 minutes before rt-PA administration.[4] At 4 hours after MCA occlusion, to assess RAP, 21 mice were randomized to receive solvent or 1 or 2 mg/kg RAP following rt-PA administration, and were then euthanized at 6 hours after MCA occlusion. Two mice were excluded from the analysis because of failure of injection, leaving group sizes of $n = 5$ for solvent and $n = 7$ for 1 and 2 mg/kg RAP, respectively. The involvement of rt-PA proteinase activity was assessed by treatment with the same volume of inactive rt-PA (with its active site blocked by D-Phe-Pro-Arg-chloromethylketone (Calbiochem, Schwalbach, Germany)) administered at 4 hours after MCA occlusion.[4] Twelve mice at

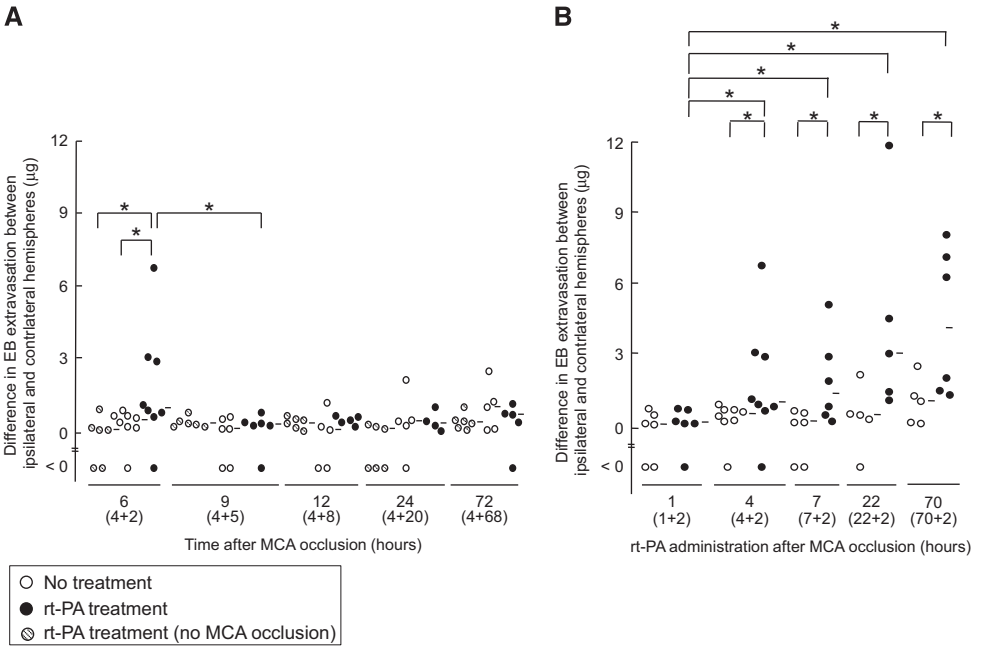

Figure 1. Effect of recombinant tissue-type plasminogen activator treatment on Evans blue extravasation in mice with middle cerebral artery occlusion. (**A**) Evans blue (EB) extravasation after different durations (6, 9, 12, 24, or 72 hours) of recombinant tissue-type plasminogen activator (rt-PA) treatment (10 mg/kg), all initiated at 4 hours after permanent middle cerebral artery (MCA) occlusion. Sham operation (hatched dots) indicates rt-PA-treated mice without MCA occlusion. (**B**) The EB extravasation after 2-hour rt-PA treatment, which was initiated 1, 4, 7, 22, or 70 hours after permanent MCA occlusion. The numbers in parentheses indicate the time points of the rt-PA treatment after MCA occlusion and the time from rt-PA treatment until euthanization. Bars represent median value. *$P < 0.05$ (Mann–Whitney *U*-test).

4 hours after MCA occlusion were randomized into two groups treated with inactivated rt-PA or solvent ($n = 6$ per group). The involvement of VEGFR-2 was assessed by treatment with SU1498 (Calbiochem), a selective inhibitor of VEGFR-2 kinase, or sunitinib (Sigma-Aldrich), a multi-targeted receptor tyrosine kinase inhibitor. For SU1498 administration, 21 mice were randomized into three groups treated with 10 or 20 mg/kg SU1498 or solvent containing dimethyl sulfoxide via intraperitoneal administration 5 minutes after rt-PA administration.[21,22] One mouse in the 10 mg/kg group died before perfusion, leaving group sizes of $n = 7$ for solvent and 20 mg/kg SU1498 and $n = 6$ for 10 mg/kg SU1498. For sunitinib administration, 30 mice were randomized into three groups treated with 10 or 20 mg/kg sunitinib or solvent containing dimethyl sulfoxide as an intravenous administration 5 minutes after rt-PA administration.[23] Two mice were excluded from the analysis because of injection failure, leaving group sizes of $n = 8$ for solvent and $n = 10$ for 10 and 20 mg/kg sunitinib. The EB was injected intravenously 2 hours before euthanization. Just before euthanization, mice were transcardially perfused with saline to wash out blood and dye. The brain was then removed, divided into hemispheres, and immersed in formamide (300 μL/hemisphere). The absorbance of formamide supernatant was measured at 650 nm.[21] Both wet and dry weights of the contralateral and ipsilateral hemispheres were measured to evaluate brain edema, as described elsewhere.[24] To assess brain water content, 10 mice were randomized into two groups with either rt-PA or solvent treatment at 4 hours after MCA occlusion followed by 6 hours until euthanization ($n = 5$ per group).

Ex vivo electron microscopic observation. To evaluate vasculature and BBB permeability at the ischemic border area, electron microscopic analysis was performed in mice with MCA occlusion. Briefly, 100 μL gold-conjugated bovine serum albumin (BSA; 10-nm particle size, 15 μg/mL, EY Laboratories, CA, USA) was injected into mice with MCA occlusion 90 minutes after rt-PA treatment via an internal carotid artery. EB was intravenously injected to identify the ischemic border areas. Under anesthesia, brains were removed and cut into small pieces such that they included EB extravasation, a marker of the penumbra. The small pieces were frozen with a high-pressure freezer system (Pact II, Leica, Wetzlar, Germany), freeze-substituted by acetone–osmium, and embedded in an epoxy resin (Quetol-812, Nissin EM, Tokyo, Japan). Ultra-thin sections (80-nm thickness) were obtained and stained with uranium acetate and lead citrate. The completed specimens were observed using a transmission electron microscope (JEM 1220, JEOL, Tokyo, Japan). We counted the number of gold-conjugated BSA particles in three sections of each group using a grid (200 mesh/inch, Veco, Eerbeek, The Netherlands). In a grid of 7.2×10^3 μm^2, a mean of 0.96 ± 0.56 vessels was observed. For electron microscopic observation, 16 mice were randomized into four groups: rt-PA at 4 hours after MCA occlusion, euthanization at 6 hours after MCA occlusion; rt-PA at 22 hours, euthanization at 24 hours; and the same schedules for controls ($n = 4$ per group).

Cell culture. The transformed mouse brain endothelial cell line bEnd.3 was used for *in vitro* studies, as described elsewhere.[4] Oxygen-glucose deprivation (OGD), which mimics ischemic stress, was applied to the cells using a combination of the Anaeropack KENKI system (Mitsubishi Gas, Tokyo, Japan) and culture in glucose-free DMEM (Dulbecco's modified Eagle's medium; Sigma-Aldrich) in the absence of fetal calf serum. After 4 hours of OGD, cells were further cultured in DMEM with 25 mmol/L glucose under normoxia for 2 or 5 hours. Control cells were cultured in DMEM with 25 mmol/L glucose for 6 or 9 hours under normoxia. The rt-PA (10 μg/mL), inactivated rt-PA (10 μg/mL), VEGF (25 ng/mL; R&D Systems, Minneapolis, MN, USA), or solvent was added to the bath medium on the completion of 4-hour OGD or normoxia.

To study the involvement of LRP, HIF-1α, and VEGF, cells were treated with 200 nmol/L RAP, 2 μg/mL anti-LRP antibody, 2 μg/mL anti-VEGF antibody (R&D), 2 μg/mL anti-VEGFR-2 antibody (sc-6251, Santa Cruz Biotechnology, Santa Cruz, CA, USA), 5 μmol/L SU1498,[25] or 100 nmol/L sunitinib 15 minutes before rt-PA administration. CAY10585, a blocker of HIF-1α accumulation, was continuously administered at a dose of 0, 3, or 10 μmol/L, starting at 12 hours before OGD and continuing until harvest.[26] The cells were treated with chetomin, an inhibitor of the binding of HIF-1α and HIF-2α to p300, at a dose of 0, 1, 10, or 100 nmol/L, starting from when OGD was initiated and continuing until harvest.[27]

Quantitative real-time polymerase chain reaction. Quantitative real-time polymerase chain reaction was performed as previously described[4] with some modifications. Total RNA prepared from cells using the TRIzol reagent (Invitrogen, Carlsbad, CA, USA) was subjected to reverse transcription (PrimeScript 1st strand cDNA Synthesis kit, Takara-Bio, Otsu, Japan) to generate cDNA. The following primers were used (Takara-Bio): 5′-ACATTGGCTCACTTCCAGAAACAC-3′ (VEGF-A forward primer, MA089111-F), 5′-GGTTGGAACCGGCATCTTTATC-3′ (VEGF-A reverse primer, MA089111-R), 5′-CATCCGTAAAGACCTCTATGCCAAC-3′ (β-actin, forward primer), and 5′-ATGGAGCCACCGATCCACA-3′ (β-actin, reverse primer). Polymerase chain reaction conditions have been previously reported.[4] β-Actin was used to normalize gene expression in all the samples. The specificity of polymerase chain reaction amplification was demonstrated by the presence of only one peak in the dissociation curve and of a single band on 2% agarose gel electrophoresis.

Preparation for western blotting. Protein levels were quantified using western blot analysis, as previously described[4,28] with some modifications. Translocation of HIF-1α into the nucleus was measured by a combination of cell fractionation and western blotting with a rabbit anti-HIF-1α monoclonal antibody (sc-1079, Santa Cruz Biotechnology).[4,28] As an internal nuclear protein control, histone deacetylase-1 was measured using a polyclonal antibody (H3284, Sigma-Aldrich). For VEGFR-2 immunoprecipitation, the supernatant was immunoprecipitated using polyclonal goat anti-mouse VEGFR-2 (R&D systems) conjugated to protein G Dynabeads (Invitrogen Dynal, Oslo, Norway), eluted with sodium dodecyl sulfate sample buffer, and subjected to sodium dodecyl sulfate-polyacrylamide gel electrophoresis. For western blotting analysis, we used antibodies against a rat anti-mouse VEGF-A_{164} (R&D Systems), mouse anti-VEGFR-2 (sc-6251, Santa Cruz Biotechnology), and rabbit anti-phospho-VEGFR-2 (Tyr-1175, 19A10, Cell Signaling Technology, Danvers, MA, USA) monoclonal antibodies, respectively.

Histologic analysis. Endocytosis *in vitro* was quantified as previously described[29] with some modifications. Briefly, bEnd.3 cells were seeded at 7.2×10^5 cells/mL onto 18-mm cover glasses, and assessed using confocal microscopy after 3 days. At 90 minutes after drug administration, the cells were incubated with fluorescein-conjugated BSA (50 μg/well; Invitrogen, USA) at 37 °C for 30 minutes. The cells were then fixed with 1% paraformaldehyde in phosphate-buffered saline, mounted with ProLong Gold Antifade Reagent containing 4′,6-diamidino-2-phenylindole (Invitrogen), and analyzed by immunofluorescence microscopy (Olympus FV1000-D; Olympus, Tokyo, Japan). Photographs were taken at $\times 100$ objective lens magnification with oil at room temperature and merged using CellSens Standard software. The number of cells was counted in nine independent fields of some slide glasses using a $\times 40$ objective lens magnification. These fields contained a mean of 10 ± 5.3 cells in the normoxia group.

Assessment of blood–brain barrier permeability in vitro. Permeability across the endothelial cell monolayer was measured using transwell units (12-mm diameter, 3.0-μm-pore polyester membrane; Corning Costar Corporation, New York, NY, USA) as previously described[30] with some modifications. Briefly, bEnd.3 cells were seeded onto a transwell insert in DMEM containing fetal calf serum at a concentration of 2×10^5 cells/mL. The lower compartment was filled with the same medium and was then cultured with inserts placed in a 12-well dish. After 10 days, cell confluence was assessed by light microscopy, and the cells were used as an *in vitro* BBB model for further experiments. Evans blue-bound albumin (EBA) prepared by dialysis (Seamless Cellulose Tubing, Small Size 30; Wako, Osaka, Japan) was added to the upper compartment after rt-PA treatment (0, 1, 3, 10, or 30 μg/mL). After 20 minutes, the concentration of EBA in the lower compartment was measured based on absorbance at 650 nm. We also assessed the transepithelial electrical resistance using a Millicell ERS-2 device (Merck Millipore, Billerica, MA, USA).

Statistical Analysis

Data are represented as mean ± s.d. values or median and range. Statistical comparisons were performed by one-way analysis of variance and Fisher's protected least significant difference (PLSD) test. Sample size was determined on the basis of the preliminary assessment of EB extravasation using groups of three mice each (Supplementary Figure 1). From the results, we observed a clear difference between the groups treated with or not treated with rt-PA at 6 hours after MCA occlusion (12 ± 9.6 μg with rt-PA and 0.74 ± 0.36 μg without rt-PA). Using these values for an expected mean difference, the necessary sample size was 4 when the power ($1 - \beta$) was 0.5. Therefore, we decided to use six animals in each group, for a power ($1 - \beta$) of 0.74. The difference between two non-parametric groups

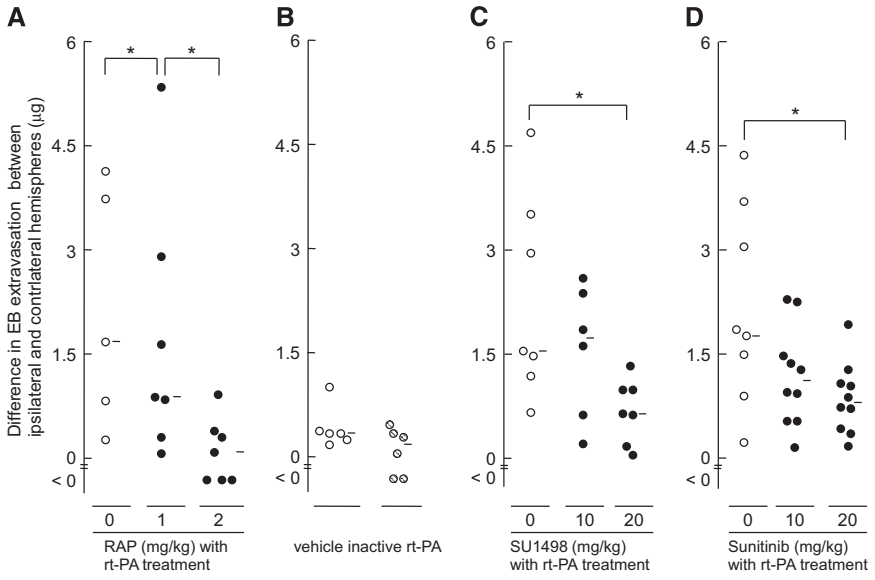

Figure 2. The effect of receptor-associated protein, inactivated recombinant tissue-type plasminogen activator, SU1498, or sunitinib on EB extravasation. The effect of receptor-associated protein (RAP; **A**), SU1498 (**C**), or sunitinib (**D**) on EB extravasation in mice treated with recombinant tissue-type plasminogen activator (rt-PA) at 4 hours after permanent middle cerebral artery (MCA) occlusion. The rt-PA or inactive rt-PA (**B**) was administered at 10 mg/kg. Vehicle indicates treatment with solvent only (**B**). The RAP was intravenously administered at 1 or 2 mg/kg, 5 minutes before rt-PA treatment. The SU1498 was intraperitoneally administered at 10 or 20 mg/kg, 5 minutes after rt-PA treatment. Sunitinib was intravenously administered at 10 or 20 mg/kg, 5 minutes after rt-PA treatment. Bars represent median values. $^*P < 0.05$ (Mann–Whitney *U*-test). EB, Evans blue; RAP, receptor-associated protein.

was analyzed by Mann–Whitney *U*-test (Figures 1 and 2). *P* values < 0.05 were considered significant.

RESULTS

Recombinant Tissue-Type Plasminogen Activator Administration Induces a Transient Increase in Blood–Brain Barrier Permeability After Middle Cerebral Artery Occlusion

The effect of intravenous injection of rt-PA on BBB permeability after permanent MCA occlusion is shown in Figure 1. In mice treated with rt-PA 4 hours after MCA occlusion, EB extravasation was markedly higher at 2 hours after treatment compared with vehicle-treated mice, whereas it was comparable at 5 hours after treatment (Figure 1A). This EB extravasation was not observed in sham-operated mice after rt-PA treatment. Furthermore, the median values (range) at doses of 0 (solvent, $n = 10$), 0.9 ($n = 6$), 3 ($n = 6$), or 10 mg/kg of rt-PA ($n = 8$) were 0.82 (< 0 to 2.8), 1.1 (0.13 to 2.1), 0.44 (< 0 to 3.4), and 3.2 (< 0 to 23), respectively. Only the 10-mg/kg dose significantly increased EB extravasation compared with the solvent group. In addition, the brain water content was $79.6 \pm 0.22\%$ and $79.6 \pm 0.24\%$ in the ipsilateral and contralateral hemispheres, respectively ($n = 5$ each), which was comparable to that of mice without rt-PA treatment ($79.6 \pm 0.47\%$ and $79.4 \pm 0.13\%$ in the ipsilateral and contralateral hemispheres, respectively; $n = 5$ each). These findings indicate that the increase in BBB permeability induced by rt-PA treatment was associated with a reversible response, but was not associated with complete BBB breakdown.

Euthanasia was performed at 2 hours after rt-PA treatment unless otherwise stated. An increase in BBB permeability was observed when rt-PA administration was delayed 4 hours or later after MCA occlusion, but not when it was administered 1 hour after MCA occlusion (Figure 1B), as also shown in our previous report.[4] These findings indicate that rt-PA has a refractory period from the onset of ischemic symptoms to the increase in BBB permeability.

Effect of a Low-Density Lipoprotein Receptor or Vascular Endothelial Growth Factor Receptor-2 Antagonist on the Increase in Blood–Brain Barrier Permeability by Recombinant Tissue-Type Plasminogen Activator Administration *In Vivo*

To explore the involvement of LDLRs and VEGF, we examined the effects of either RAP, an antagonist of LDLRs; SU1498, a selective inhibitor of VEGFR-2 kinase; or sunitinib, a multi-target inhibitor of tyrosine kinases, on BBB permeability by rt-PA administration. The EB extravasation after rt-PA administration was suppressed by treatment with RAP, SU1498, or sunitinib in a dose-dependent manner in mice treated with rt-PA 4 hours after MCA occlusion (Figures 2A, 2C, and 2D). Inactivated rt-PA did not alter EB extravasation (Figure 2B). These findings indicated that LDLRs and VEGF-2 receptor activation were involved in the increase in BBB permeability by rt-PA treatment after ischemia, and that their protease activity was necessary to this involvement.

Delayed Tissue-Type Plasminogen Activator Treatment Induces the Expression of Vascular Endothelial Growth Factor via Nuclear Translocation of HIF-1α in a Mouse Brain Endothelial Cell Line, bEnd.3

We evaluated the effect of OGD, a model of ischemia, and rt-PA treatment on VEGF expression in a transformed mouse brain endothelial cell line, bEnd.3. The harvest for evaluation was performed at 2 hours after rt-PA treatment unless otherwise stated. Four hours of OGD followed by 2 hours of normoxia decreased cell viability to $89 \pm 1.2\%$ of normoxic control levels determined by lactate dehydrogenase assay ($n = 6$), whereas additional rt-PA treatment did not alter cell viability ($89 \pm 1.7\%$). In addition, cell viability was comparable when the cells were incubated with rt-PA ($93 \pm 1.8\%$ of control levels) or without rt-PA ($94 \pm 0.7\%$) over 5 hours under normoxia after 4 hours of normoxia without rt-PA, as well as when cells were incubated with rt-PA ($80 \pm 2.0\%$ of control levels) or without rt-PA ($82 \pm 1.0\%$) over 20 hours under normoxia after 4 hours of normoxia without rt-PA.

These results indicate that rt-PA at this dose did not influence the cell viability of bEnd.3 cells.

The VEGF messenger RNA (mRNA) was significantly upregulated by 4-hour OGD alone and decreased following subsequent normoxia, reaching its basal level 5 hours after the restoration of normoxia (Figure 3A). The rt-PA administration after 4-hour OGD significantly enhanced VEGF mRNA expression 2 hours after the end of OGD, which again decreased to basal levels at 5 hours after the restoration of normoxia. Under normoxic conditions, VEGF mRNA levels were not altered at 2, 5, or 20 hours after rt-PA treatment (1.1 ± 0.17-fold increase ($n = 5$), 0.89 ± 0.25-fold increase ($n = 5$), or 1.2 ± 0.13-fold increase ($n = 3$), respectively). After 4-hour OGD followed by 2-hour normoxia, neither treatment with inactivated rt-PA nor RAP pretreatment with active t-PA increased the expression of VEGF mRNA (Figure 3B).

Consistently, VEGF protein levels in b.End3 cells were significantly increased by 2-hour rt-PA treatment under normoxia after 4-hour OGD ($P < 0.05$ versus OGD, Figure 3C), which was inhibited by pretreatment with RAP. Treatment with inactivated rt-PA did not increase VEGF protein level. Under normoxic conditions, VEGF protein levels were not altered 2, 5, or 20 hours after rt-PA treatment (1.1 ± 0.21-fold increase ($n = 5$), 0.84 ± 0.14-fold increase ($n = 6$), or 0.86 ± 0.30-fold increase ($n = 3$), respectively). Although VEGFR-2 protein levels were not altered by the rt-PA treatment, the phosphorylation of VEGFR-2 Tyr-1175 was significantly increased ($P < 0.01$ versus OGD, Figure 3D). This increase was also suppressed by pretreatment with RAP (Figure 3D).

Induction of VEGF expression during hypoxia in endothelial cells has been reported to result from the accumulation of HIF-1α,[17] which has a major role in the transcriptional activation of genes.[18,19] We therefore analyzed the effect of rt-PA after ischemia on HIF-1α levels in bEnd.3 cells. Two-hour rt-PA treatment under normoxia after 4-hour OGD did not alter HIF-1α mRNA levels (1.3 ± 0.33-fold increase, $n = 4$), but it enhanced nuclear accumulation of HIF-1α in bEnd.3 cells (Figure 3E). This enhancement was also suppressed by RAP pretreatment, and treatment with inactivated rt-PA did not enhance the nuclear accumulation of HIF-1α by OGD (Figure 3E). The rt-PA treatment also did not alter nuclear accumulation of HIF-1α under normoxic conditions (1.2 ± 0.16-fold increase, $n = 6$). However, the increase in VEGF mRNA by rt-PA treatment was not altered upon inhibition of HIF-1 accumulation by CAY10585 (Figure 3F) and chetomin (data not shown). Taken together, these data suggest that rt-PA treatment promoted VEGF induction in endothelial cells through a mechanism other than enhancement of HIF-1α accumulation.

The Increase in Endothelial Endocytosis and Blood–Brain Barrier Permeability by Recombinant Tissue-Type Plasminogen Activator Occurs via Lipoprotein Receptor-Related Protein and Requires its Protease Activity in b.End3 Cells

We next investigated translocation of fluorescein-conjugated BSA into bEnd.3 cells. Under normoxia, fluorescein-conjugated BSA was translocated very little in bEnd.3 cells both with and without

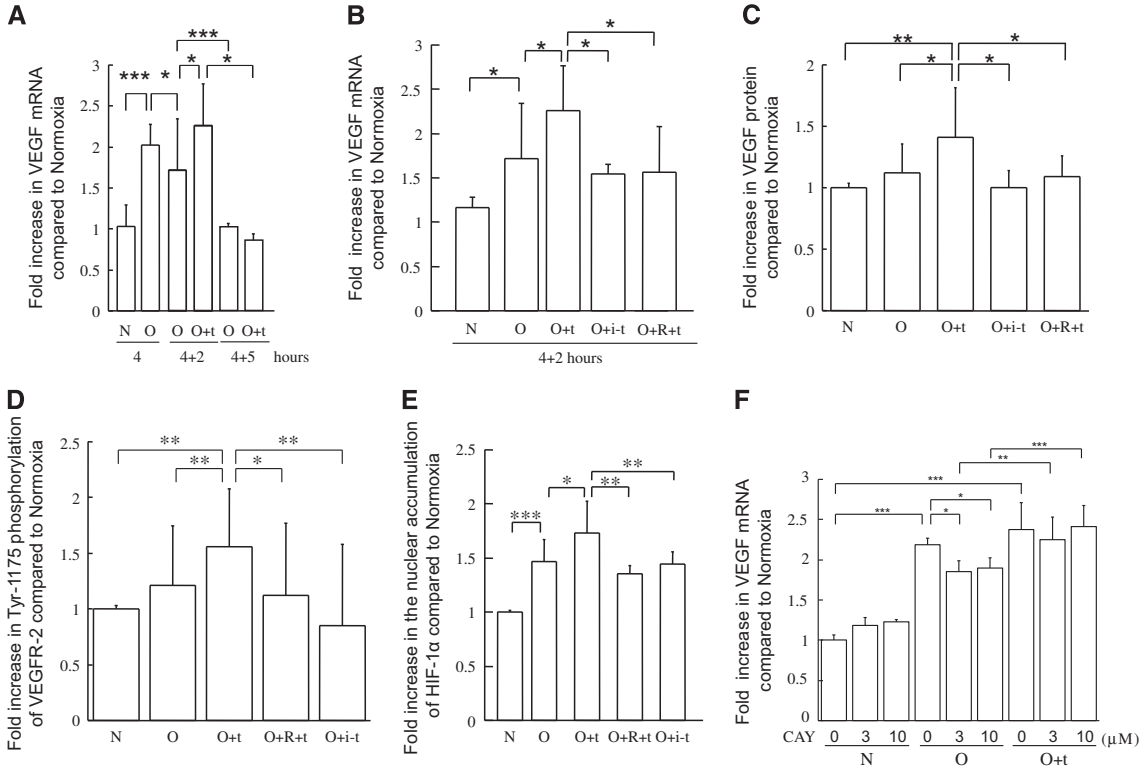

Figure 3. Effects of recombinant tissue-type plasminogen activator treatment and oxygen-glucose deprivation on secretion of vascular endothelial growth factor and nuclear accumulation of hypoxia-inducible factor-1 alpha in bEnd.3 cells. The time course of vascular endothelial growth factor (VEGF) mRNA expression in bEnd.3 cells treated with 4 hours of oxygen-glucose deprivation (OGD) alone or followed by up to 5 hours of normoxia in the absence or presence of recombinant tissue-type plasminogen activator (rt-PA; **A**). (**B**–**F**): Expression of VEGF mRNA (**B**, **F**) or protein (**C**), phosphorylated VEGF receptor-2 (VEGFR-2; **D**), and nuclear accumulation of hypoxia-inducible factor-1 alpha (HIF-1α; **E**) in bEnd.3 cells after 4-hour OGD followed by 2 hours of normoxia. Quantitative data in **A** and **B** are indicated as fold increase compared with the 4-hour normoxia condition without treatment, and quantitative data in **C**–**F** are indicated as fold increase compared with the normoxia group without treatment. Treatments are indicated as follows: OGD, O; normoxia, N; treatment with rt-PA, +t; treatment with active site-blocked rt-PA, +i-t; receptor-associated protein pretreatment, +R; and CAY10585, CAY. Data represent mean ± s.d. of 4 to 17 experiments; $^{*}P < 0.05$, $^{**}P < 0.01$, and $^{***}P < 0.001$. mRNA, messenger RNA.

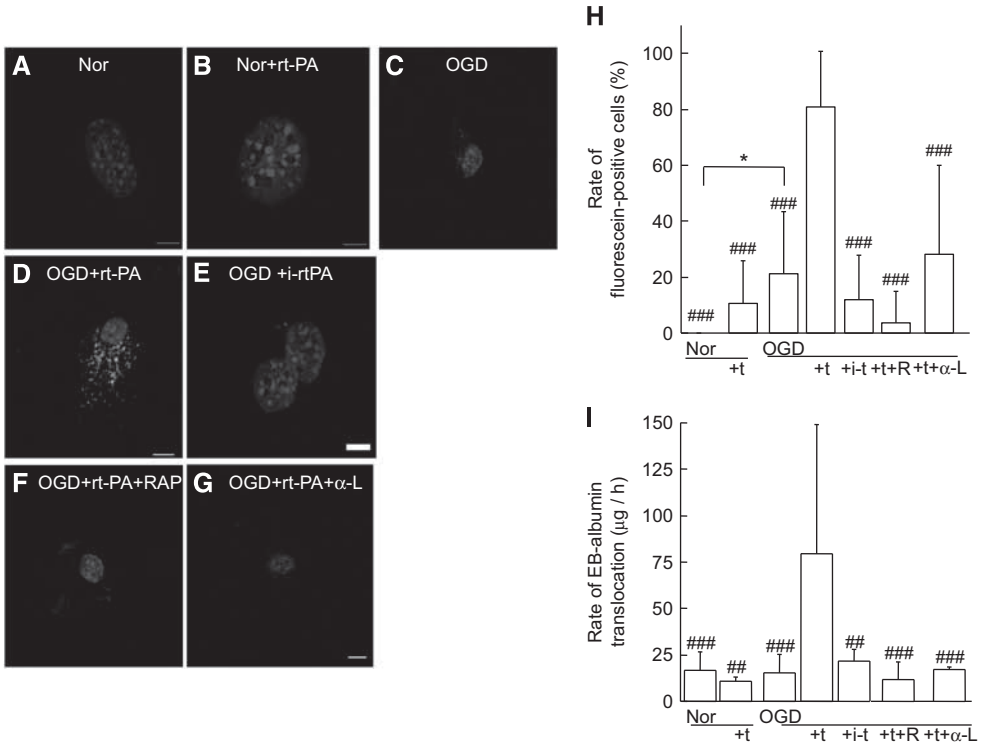

Figure 4. Recombinant tissue-type plasminogen activator treatment under ischemic conditions causes endocytosis and Evans blue (EB) extravasation in brain-derived endothelial cells. Representative images of bEnd.3 cells under normoxia (Nor) for 6 hours (**A**, **B**). Normoxic control cells (**A**) and recombinant tissue-type plasminogen activator (rt-PA)-treated cells (10 μg/mL) in the absence of hypoxia (**B**) are shown. The rt-PA was administered after 4 hours of normoxia, and cells were harvested after two more hours under normoxic conditions (**B**). Representative images under ischemic conditions with 4-hour oxygen-glucose deprivation (OGD) followed by 2-hour normoxia without (**C**) or with rt-PA treatment (**D**). The OGD with rt-PA induced translocation of fluorescein-conjugated bovine serum albumin (BSA; green) into the cytoplasm but not nucleus (**D**), which was inhibited by pretreatment with receptor-associated protein (RAP; **F**) or anti-low-density lipoprotein receptor-related protein (LRP) antibody (**G**). Treatment with inactive rt-PA (i-rt-PA) did not affect translocation (**E**). Nuclei were stained with mounting medium containing 4′,6 diamidino-2-phenylindole (DAPI, blue). Scale bars indicate 10 μm. (**H**) The ratio of fluorescein-positive cells is indicated ($n = 9$). (**I**) The effect of rt-PA on the translocation of EB-albumin through a monolayer of bEnd.3 cells was recorded. The rt-PA was administered to the upper chamber, and permeability was assessed. The treatments are indicated as follows: normoxia, Nor; oxygen-glucose deprivation, OGD; rt-PA, +t; active site-blocked rt-PA, +i-t; pretreatment with RAP, +R; and pretreatment with anti-low-density lipoprotein receptor-related protein antibody, +α-L. Bars represent median values. Columns and error bars represent mean+s.d. ($n = 3$ to 9). $^{*}P < 0.05$ (Fisher's protected least significant difference (PLSD) test). $^{\#\#}P < 0.01$, $^{\#\#\#}P < 0.001$ (versus OGD+rt-PA; Fisher's PLSD test).

rt-PA treatment (Figures 4A and 4B). Fluorescein positivity was slightly increased by treatment with OGD alone (Figure 4C), whereas it was prominent in cytoplasm but absent in the nucleus in bEnd.3 cells treated with t-PA in addition to OGD exposure (Figures 4D and 4H). Treatment with inactive rt-PA after OGD did not alter BSA translocation (Figure 4E). The RAP treatment (Figure 4F) or LRP-neutralizing antibody (Figure 4G) suppressed the marked translocation induced after rt-PA treatment in addition to OGD.

In a transwell system, the extravasation of EBA through a bEnd.3 monolayer was not affected by either treatment with rt-PA or OGD. However, their combination significantly increased EBA extravasation in an rt-PA-dose-dependent manner (at 10 μg/mL, $P < 0.001$ versus OGD), which was suppressed by either pretreatment with RAP or LRP-neutralizing antibody (Figure 4I). Furthermore, EBA extravasation on treatment with inactivated rt-PA was comparable to treatment with OGD alone. These findings suggested that the increase in extravasation by rt-PA on a bEnd.3 monolayer also occurred via acceleration of transcellular transport, which was induced through LRP activation and required proteolytic activity of rt-PA. Transepithelial electrical resistance was unchanged by treatment with rt-PA and/or OGD (1.1 ± 0.12-fold increase for normoxia with rt-PA, 0.93 ± 0.28-fold increase for OGD alone, and 1.3 ± 0.42-fold increase for OGD with rt-PA, respectively ($n = 3$)).

Involvement of Secreted Vascular Endothelial Growth Factor/Vascular Endothelial Growth Factor Receptor-2 in Delayed Recombinant Tissue-Type Plasminogen Activator Treatment-Induced Bovine Serum Albumin Translocation

To explore the functional role of the VEGF secretion prompted by rt-PA under ischemia in the activation of endothelial endocytosis, we studied the effects of VEGF inhibition on the translocation of fluorescein-conjugated BSA (Figures 5A–I) and the phosphorylation of VEGFR-2 (Figure 5J) in bEnd.3 cells. The marked translocation of fluorescein-conjugated BSA induced by rt-PA treatment after OGD was inhibited by administration of an anti-VEGF monoclonal antibody (Figure 5A); anti-VEGFR-2 monoclonal antibody (Figure 5B); SU1498, a selective inhibitor of VEGFR-2 kinase (Figure 5C); or sunitinib, a multi-target inhibitor of tyrosine kinases with growth factor receptors (Figure 5D). Furthermore, VEGF treatment induced marked translocation of fluorescein-conjugated BSA in the cytoplasm (Figure 5E). In addition, the increased Tyr-1175 phosphorylation of VEGFR-2 observed upon rt-PA treatment after OGD was suppressed by anti-VEGF antibody, anti-VEGFR-2 antibody, or sunitinib (Figure 5J). In the transwell

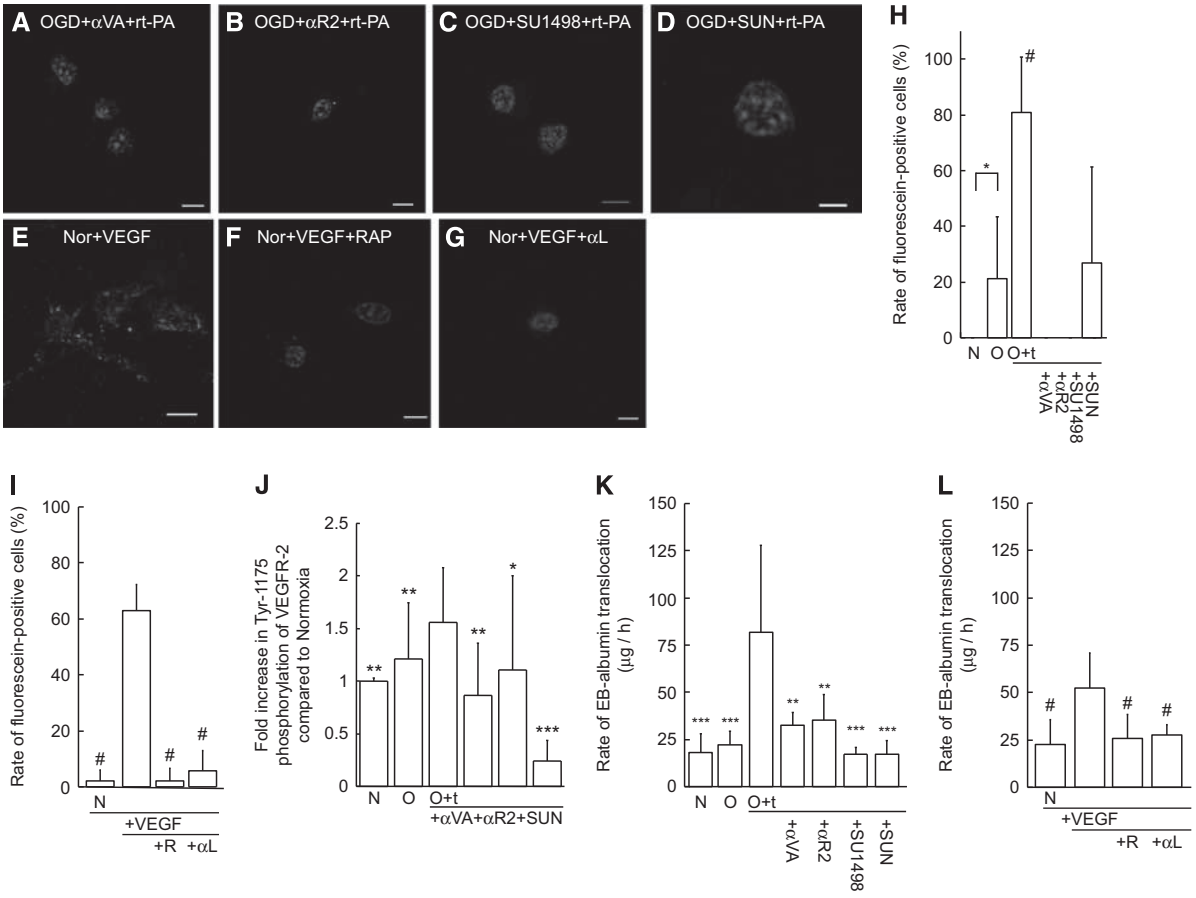

Figure 5. Inhibitory effects of vascular endothelial growth factor (VEGF) on endocytosis and phosphorylation of VEGF receptor-2 in bEnd.3 cells. (**A**–**G**) Representative images of the translocation of fluorescein-conjugated bovine serum albumin (BSA) in bEnd.3 cells under the following conditions: rt-PA under oxygen-glucose deprivation (OGD) and pretreatment with anti-vascular endothelial growth factor (VEGF) monoclonal antibody (**A**); anti-VEGF receptor-2 (VEGFR-2) monoclonal antibody (**B**); SU1498 (**C**); sunitinib (SUN; **D**); or VEGF (25 ng/mL) alone (**E**), with receptor-associated protein (RAP) pretreatment (**F**), or with anti-low-density lipoprotein receptor-related protein (LRP) antibody pretreatment (**G**) under normoxia. The rate of fluorescein-positive cells indicates the inhibitory effect on induction by rt-PA under OGD (**H**) and by VEGF under normoxia (**I**). Effect of VEGF inhibition on VEGFR-2 phosphorylation (**J**). Effect of VEGF inhibition on the translocation of Evans blue-albumin through a monolayer of bEnd.3 cells treated with rt-PA under OGD (**K**). Effect of LRP inhibition on the translocation by VEGF under normoxia (**L**). All the quantitative data are indicated as fold increase compared with the normoxia group without treatment. Samples derived from the same experiment and blots were processed in parallel. Treatments are indicated as follows: normoxia, N; OGD, O; treatment with rt-PA, +t; pretreatment with anti-VEGF monoclonal antibody, +*α*VA; anti-VEGFR-2 monoclonal antibody, +*α*R2; sunitinib, +SUN; VEGF, +VEGF; RAP, +R; and anti-LRP antibody, +*α*L. Data represent mean ± s.d. of 4 to 17 experiments; $^{*}P < 0.05$, $^{**}P < 0.01$, and $^{***}P < 0.001$ (versus OGD+t-PA). $^{\#}P < 0.05$ (versus Nor+VEGF).

system, the increased extravasation of EBA through the bEnd.3 monolayer observed upon rt-PA treatment after OGD was suppressed by administration of an anti-VEGF monoclonal antibody, anti-VEGFR-2 monoclonal antibody, SU1498, or sunitinib (Figure 5K). In addition, RAP or LRP-neutralizing antibody suppressed the VEGF-induced translocation of both fluorescein-conjugated BSA (Figures 5F, 5G, and 5I) and EBA in the transwell system (Figure 5L). Furthermore, VEGF induced a small (1.2-fold) but significant increase in LRP mRNA level (data not shown). These findings indicate that not only rt-PA but also secreted VEGF may activate LRP, which may act as a scavenger receptor for aberrant proteins.

Delayed Recombinant Tissue-Type Plasminogen Activator Treatment Induces Translocation of Bovine Serum Albumin into Endothelial Cells *In Vivo*

Next, we performed electron microscopic analysis at the region of increased BBB permeability (Figure 6H). At 6 hours after MCA occlusion, the ultrastructure of the endothelium and vasculature in the EB-positive region was comparable with that of naive brain regions in mice both without (Figures 6A–C) and with rt-PA treatment (Figures 6D, 6E, and Supplementary Figure 2A). Gold-labeled BSA was present only at the vascular lumen of mice without rt-PA treatment, whereas it was present both at the vascular lumen and within endothelial cells in mice with rt-PA treatment (Figure 6E and Supplementary Figure 2A). Vessels containing BSA were observed more frequently in mice with rt-PA treatment than those without rt-PA (Figure 6F). In addition, gold-labeled BSA was distributed inside of the lumen in mice without rt-PA treatment, whereas it was also present inside endothelial cells, extracellular matrix, and extravascular space in those with rt-PA treatment (Figure 6G). The region of increased EB extravasation was more than 3 mm from the MCA occlusion point (Figure 6H). We observed primarily bleeding at the site of surgical occlusion, with hardly any intracranial hemorrhage induced by rt-PA.

At 24 hours after MCA occlusion, the membrane structure of endothelial cells and cells around the vasculature was altered (Supplementary Figure 2C). The basal lamina demonstrated a fissure (black arrowheads in Supplementary Figures 2C and 2E).

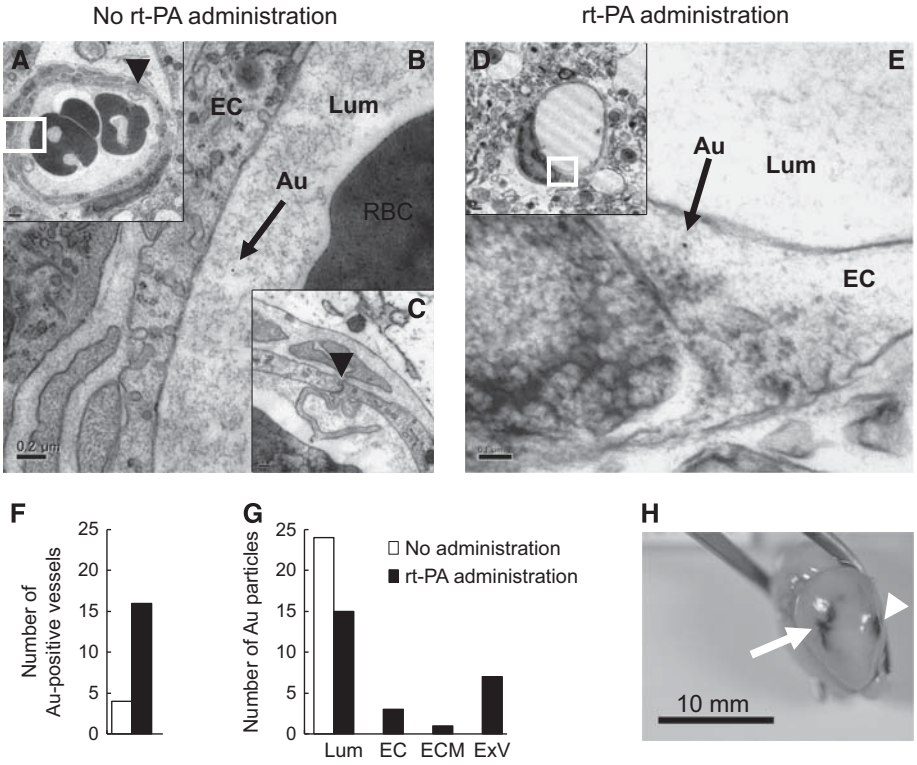

Figure 6. Vascular structure and location of gold-conjugated bovine serum albumin after recombinant tissue-type plasminogen activator treatment. Representative transmission electron microscopy images at the ischemic border area 6 hours after middle cerebral artery (MCA) occlusion in mice without (**A**–**C**) or with recombinant tissue-type plasminogen activator (rt-PA) treatment (**D**, **E**), which was administered at 4 hours after MCA occlusion. The photographs in **B** and **E** show enlarged images of the small squares in **A** and **D**, respectively. The black arrows indicate gold-conjugated bovine serum albumin (BSA; **B**, **E**). The black arrowheads in **A** and **C** indicate an endothelial tight junction, with the photograph in **C** showing a middle-power field of **A**. (**F**, **G**) Quantitative analysis of gold-conjugated BSA is shown. Vessels containing gold-conjugated BSA were more frequent in mice with rt-PA treatment (closed columns) compared with those without rt-PA treatment (open columns; **F**). Gold-conjugated BSA was absent from the endothelial cells, extracellular matrix, and extravascular space in mice without rt-PA (**G**). (**H**) A representative photograph of a brain after perfusion is shown. The white arrow in **H** indicates the region of increased EB extravasation. The white arrowhead in **H** indicates the MCA occlusion point. Bars indicate 0.1 μm in **E**, 0.2 μm in **B** and **C**, 0.5 μm in **D**, 1 μm in **A**, and 10 mm in **H**. Au, gold-conjugated BSA; EC, endothelial cell; ECM, extracellular matrix; ExV, extravascular space; Lum, lumen; RBC, red blood cell.

However, red blood cells were present in the vascular lumen, and the structure of the vasculature was retained in the ischemic border area (Supplementary Figure 2C). These findings suggest that delayed rt-PA treatment increased extravasation of BSA in the early period after MCA occlusion by additional acceleration of transcellular transport rather than by degradation of vascular structures.

DISCUSSION

Recombinant Tissue-Type Plasminogen Activator Administration Increases Reversible Blood–Brain Barrier Permeability after Middle Cerebral Artery Occlusion

In our murine stroke model, delayed rt-PA treatment beyond 4 hours after MCA occlusion enhanced BBB permeability over 2 hours after rt-PA treatment. Notably, since vascular ultrastructure including the extracellular matrix and peripheral neurons appeared intact 4 hours after MCA occlusion, permeability did not appear to increase in the absence of rt-PA treatment. Furthermore, 24 hours after MCA occlusion, the basal lamina of the vascular ultrastructure had already degenerated, but BBB permeability showed no increase in EB extravasation in the absence of rt-PA treatment. These findings imply the existence of active mechanisms underlying the increase in BBB permeability regardless of BBB breakdown.

Recombinant Tissue-Type Plasminogen Activator Enhances Blood–Brain Barrier Permeability via Lipoprotein Receptor-Related Protein, Which Requires its Protease Activity

The mechanism underlying the increase in BBB permeability by rt-PA remains controversial. In this study, no increase in BBB permeability was induced by treatment with inactivated rt-PA, which is consistent with previous observations.[4,7,8] Considering that ischemic stress induces LRP in endothelial cells in ischemic stroke[4] and that administration of anti-LRP antibody reduced the increase in permeability by rt-PA in a transwell system, the effect of rt-PA on BBB permeability appears to occur via LRP. Proteolytic activity of rt-PA and LRP activation both seemed to be necessary for the increase in BBB permeability. Thus, it is possible that rt-PA increases BBB permeability through multiple pathways including LRP activation and/or degradation of other substrates.

Recombinant Tissue-Type Plasminogen Activator Treatment Induces Vascular Endothelial Growth Factor in Endothelial Cells

The VEGF increases vascular permeability via activation of VEGFR-2.[31,32] In the present study, we found that either SU1498 or sunitinib suppressed the transient increase in BBB permeability

induced by delayed rt-PA treatment in mice. We also showed that rt-PA treatment under ischemic stress upregulated VEGF, which peaked at 6 hours, and subsequent activation of VEGFR-2 tyrosine kinase activity. In addition, both VEGF induction and subsequent VEGFR-2 activation were suppressed by RAP, indicating that rt-PA may also act upstream of the VEGF pathway through LRP activation. However, rt-PA treatment after ischemia did not enhance the expression of VEGF through nuclear accumulation of HIF-1α in endothelial cells. Identifying the novel mechanism that does underlie this effect of rt-PA on VEGF remains a question for further investigation.

Recombinant Tissue-Type Plasminogen Activator Activates Endocytosis in Endothelial Cells Under Ischemic Stress Through a Vascular Endothelial Growth Factor/Vascular Endothelial Growth Factor Receptor-2 Pathway

Two possible active mechanisms may affect BBB permeability: an acceleration of transcellular transport of endothelial cells and reversible weakening of tight junctions between endothelial cells. Vascular endothelial growth factor is known to accelerate both mechanisms.[14,15] In the present study, rt-PA treatment accelerated the translocation of labeled BSA into the cytoplasm of endothelial cells under ischemic conditions both *in vitro* and *in vivo*. Furthermore, the translocation of BSA after rt-PA treatment in cultured endothelial cells was suppressed by the neutralization of LRP, VEGF, or VEGFR-2 or inhibition of tyrosine kinase activity. BSA translocation was also induced by VEGF treatment, which is consistent with a previous report that VEGFR-2 undergoes endocytosis triggered by VEGF binding in endothelial cells.[33] In addition, the acceleration of EBA translocation through a bEnd.3 monolayer by rt-PA was associated with VEGF/VEGFR-2 signaling without reduction of transepithelial electrical resistance. These findings indicate that rt-PA is likely to activate endocytosis and subsequent transcellular transport via the VEGF/VEGFR-2 pathway. Therefore, the acceleration of transcellular transport may be involved in the increase in BBB permeability induced by delayed treatment of rt-PA, at least in part, although the reversible weakening of tight junctions is also a potential factor in the increase in BBB permeability.

Lipoprotein Receptor-Related Protein is Involved in Multiple Processes in the Recombinant Tissue-Type Plasminogen Activator-Induced Increase in Blood–Brain Barrier Permeability

We demonstrated that VEGF-activated endocytosis was suppressed by the inhibition of LRP, indicating that LRP is involved not only as a receptor of rt-PA that induces VEGF expression but also in the endocytic reaction induced by VEGF. As LRP is known to participate in endocytosis of extracellular proteins as a scavenger receptor,[34] LRP is likely to contribute directly to phagocytic vesicle formation triggered by VEGF. As these phagocytic vesicles can also include proteins on the endothelial cell surface together with other proteins distributed on and near the cell membrane, the upregulation of transcellular transport may accelerate the extravasation of rt-PA and plasminogen into the parenchyma and subsequent degradation of ECM and serious hemorrhage.[4,21] Extravasation of plasminogen will be examined in follow-up studies.

Experimental Limitations

Here, rt-PA at a dose of 10 mg/kg was used in mice with MCA occlusion, which is higher than the clinical dose of 0.9 mg/kg in humans. The dosage of 10 mg/kg rt-PA, but neither 0.9 nor 3 mg/kg, significantly increased EB extravasation. Thus, a dosage of 10 mg/kg is necessary to assess the effect of rt-PA on the EB extravasation in mice with permanent MCA occlusion. This dose was chosen on the basis of the report by Lijnen *et al*[35] that murine plasma clots have more than 30-fold higher resistance to lysis with autologous t-PA than human plasma clots. In addition, our previous studies also demonstrated that 8 mg/kg rt-PA caused a reduction in plasma alpha2-antiplasmin without fibrinogen reduction,[36] while extensive fibrinogen breakdown only occurs in association with the complete depletion of alpha2-antiplasmin in patients with rt-PA treatment.[37] The rt-PA at a dose of 10 mg/kg induced bleeding similar to that observed using a dose of 8 mg/kg after MCA occlusion (data not shown). Although the vehicle contained a higher dose of L-arginine and Tween 80 than the clinical dose, it did not alter EB extravasation in sham-operated mice (Figure 1A). In our *in vitro* study, the exposure of cells to rt-PA did not alter the viability from control levels at a dose of 10 μg/mL over 20 hours, and the activity in the medium under normoxic conditions was reduced by $2.9 \pm 2.9\%$ ($n = 6$) from initial values. It seems more likely that rt-PA may be neutralized by PAI-1 secreted from endothelial cells or be inactivated by the condition of neutral pH. Although we used bEnd.3, an immortalized cell line, for *in vitro* studies, its signaling would be expected to be comparable to that of primary endothelial cells. Further experiments using primary cells from mice and humans are required to clarify this question.

Increase in BBB permeability because of rt-PA alone was enhanced by co-treatment with plasminogen.[8] In addition, rt-PA treatment did not alter the rate of hemorrhage associated with stroke in mice deficient in plasminogen.[38] Considering that hemorrhage is thought to occur downstream of the increase in BBB permeability, these findings also suggested involvement of plasminogen in BBB permeability.[7,38] Our current experiments demonstrated a mechanism of increased BBB permeability via LRP-1 and VEGF pathways activations. However, it remains possible that plasminogen is also involved in the increase in BBB permeability, as plasminogen can bind to lysine residues on

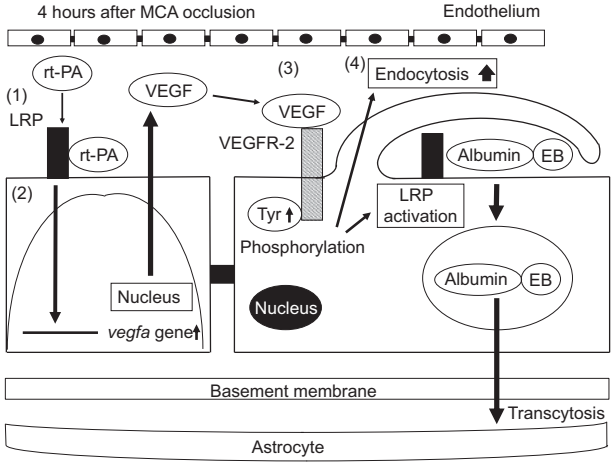

Figure 7. Schematic mechanisms of the increase in blood–brain barrier permeability by recombinant tissue-type plasminogen activator treatment after ischemic stroke. Recombinant tissue-type plasminogen activator (rt-PA) activates low-density lipoprotein receptor-related protein (LRP), which is upregulated in endothelial cells by ischemic stress (1). The activation of LRP induces the enhanced accumulation of hypoxia-inducible factor-1 alpha (HIF-1α) in the nucleus. However, the transcriptional upregulation of vascular endothelial growth factor (VEGF) by LRP activation was not induced through the enhancement of HIF-1α accumulation (2). Secreted VEGF binds to VEGF receptor-2 (VEGFR-2) on the surface of endothelial cells through an autocrine mechanism and induces its phosphorylation (3). The activation of VEGFR-2 leads to an increase in endocytosis and to the activation of LRP, resulting in enhanced blood–brain barrier (BBB) permeability by endocytosis and subsequent transcellular transport of proteins into cerebroparenchyma (4).

the cell surface,[39] which are derived from bovine serum in culture. Further experiments are required to clarify this possibility.

The present study does not provide direct evidence for involvement of exocytosis in EB extravasation. Endothelial endocytosis may be unrelated to BBB opening and the increase in permeability may occur mainly via weakening of endothelial–endothelial cell junctions, which may not necessarily involve physical breakdown, but may rather be a regulated event. Supporting this possibility, electron microscopy analysis revealed vesicular transcytosis in endothelial cells in mice without obvious tight-junction defects.[40] To clarify the possibility that permeability is associated with transcytosis, further observation of whether abluminal membrane-connected vesicles contain gold-conjugated BSA is required.

In conclusion, the present series of experiments demonstrated that delayed rt-PA treatment after ischemic stroke transiently enhanced BBB permeability, and that LDLRs and VEGF/VEGFR-2 were involved in this process. These findings suggest that the t-PA–LRP–VEGF pathway is a critical factor affecting BBB permeability, at least in part, after delayed rt-PA treatment and subsequent endothelial transcellular transport in the event of ischemic stroke (Figure 7).

AUTHOR CONTRIBUTIONS

YS designed and performed the research. NN performed the middle cerebral artery occlusion studies. KY performed the mRNA studies. KH administered the drugs and performed electron microscopy. YM performed the electron microscopy. KU was the supervisor.

DISCLOSURE/CONFLICT OF INTEREST

The authors declare no conflict of interest.

ACKNOWLEDGMENTS

The authors are grateful to Ms. Ayami Hori (Hamamatsu University School of Medicine) for excellent technical assistance.

REFERENCES

1 Wang YF, Tsirka SE, Strickland S, Stieg PE, Soriano SG, Lipton SA. Tissue plasminogen activator (tPA) increases neuronal damage after focal cerebral ischemia in wild-type and tPA-deficient mice. *Nat Med* 1998; **4**: 228–231.
2 Nicole O, Docagne F, Ali C, Margaill I, Carmeliet P, MacKenzie ET *et al.* The proteolytic activity of tissue-plasminogen activator enhances NMDA receptor-mediated signaling. *Nat Med* 2001; **7**: 59–64.
3 Nagai N, De Mol M, Lijnen HR, Carmeliet P, Collen D. Role of plasminogen system components in focal cerebral ischemic infarction: a gene targeting and gene transfer study in mice. *Circulation* 1999; **99**: 2440–2444.
4 Suzuki Y, Nagai N, Yamakawa K, Kawakami J, Lijnen HR, Umemura K. Tissue-type plasminogen activator (t-PA) induces stromelysin-1 (MMP-3) in endothelial cells through activation of lipoprotein receptor-related protein. *Blood* 2009; **114**: 3352–3358.
5 Benchenane K, Berezowski V, Ali C, Fernández-Monreal M, López-Atalaya JP, Brillault J *et al.* Tissue-type plasminogen activator crosses the intact blood-brain barrier by low-density lipoprotein receptor-related protein-mediated transcytosis. *Circulation* 2005; **111**: 2241–2249.
6 Su EJ, Fredriksson L, Geyer M, Folestad E, Cale J, Andrae J *et al.* Activation of PDGF-CC by tissue plasminogen activator impairs blood-brain barrier integrity during ischemic stroke. *Nat Med* 2008; **14**: 731–737.
7 Yepes M, Sandkvist M, Moore EG, Bugge TH, Strickland DK, Lawrence DA. Tissue-type plasminogen activator induces opening of the blood–brain barrier via the LDL receptor-related protein. *J Clin Invest* 2003; **112**: 1533–1540.
8 Niego B, Freeman R, Puschmann TB, Turnley AM, Medcalf RL. Plasmin-mediated activation of the Rho kinase pathway in astrocytes. *Blood* 2012; **119**: 4752–4761.
9 Niego B, Medcalf RL. Plasmin-dependent modulation of the blood-brain barrier: a major consideration during tPA-induced thrombolysis? *J Cereb Blood Flow Metab* 2014; **34**: 1283–1296.
10 Herz J, Hamann U, Rogne S, Myklebost O, Gausepohl H, Stanley KK. Surface location and high affinity for calcium of a 500-kd liver membrane protein closely related to the LDL-receptor suggest a physiological role as lipoprotein receptor. *EMBO J* 1988; **7**: 4119–4127.
11 Bu G, Williams S, Strickland DK, Schwartz AL. Low density lipoprotein receptor-related protein/alpha 2-macroglobulin receptor is an hepatic receptor for tissue-type plasminogen activator. *Proc Natl Acad Sci USA* 1992; **89**: 7427–7431.
12 López-Atalaya JP, Roussel BD, Ali C, Maubert E, Petersen KU, Berezowski Velli R *et al.* Recombinant Desmodus rotundus salivary plasminogen activator crosses the blood-brain barrier through a low-density lipoprotein receptor-related protein-dependent mechanism without exerting neurotoxic effects. *Stroke* 2007; **38**: 1036–1043.
13 Roux F, Couraud PO. Rat brain endothelial cell lines for the study of blood-brain barrier permeability and transport functions. *Cell Mol Neurobiol* 2005; **25**: 41–58.
14 Fischer S, Wobben M, Marti HH, Renz D, Schaper W. Hypoxia-induced hyperpermeability in brain microvessel endothelial cells involves VEGF-mediated changes in the expression of zonula occludens-1. *Microvasc Res* 2002; **63**: 70–80.
15 Horowitz A, Seerapu HR. Regulation of VEGF signaling by membrane traffic. *Cell Sig* 2012; **24**: 1810–1820.
16 Abumiya T, Yokota C, Kuge Y, Minematsu K. Aggravation of hemorrhagic transformation by early intraarterial infusion of low-dose vascular endothelial growth factor after transient focal cerebral ischemia in rats. *Brain Res* 2005; **1049**: 95–103.
17 Namiki A, Brogi E, Kearney M, Kim EA, Wu T, Couffinhal T *et al.* Hypoxia induces vascular endothelial growth factor in cultured human endothelial cells. *J Biol Chem* 1995; **270**: 31189–31195.
18 Semenza GL. HIF-1: upstream and downstream of cancer metabolism. *Curr Opin Genet Dev* 2010; **20**: 51–56.
19 Rey S, Semenza GL. Hypoxia-inducible factor-1-dependent mechanisms of vascularization and vascular remodelling. *Cardiovasc Res* 2010; **86**: 236–242.
20 Nagai N, Suzuki Y, Van Hoef B, Lijnen HR, Collen D. Effects of plasminogen activator inhibitor-1 on ischemic brain injury in permanent and thrombotic middle cerebral artery occlusion models in mice. *J Thromb Haemost* 2005; **3**: 1379–1384.
21 Kanazawa M, Igarashi H, Kawamura K, Takahashi T, Kakita A, Takahashi H *et al.* Inhibition of VEGF signaling pathway attenuates hemorrhage after tPA treatment. *J Cereb Blood Flow Metab* 2011; **31**: 1461–1474.
22 Ho VC, Duan LJ, Cronin C, Liang BT, Fong GH. Elevated vascular endothelial growth factor receptor-2 abundance contributes to increased angiogenesis in vascular endothelial growth factor receptor-1–deficient mice. *Circulation* 2012; **126**: 741–752.
23 Tang SC, Lagas JS, Lankheet NA, Poller B, Hillebrand MJ, Rosing H *et al.* Brain accumulation of sunitinib is restricted by P-glycoprotein (ABCB1) and breast cancer resistance protein (ABCG2) and can be enhanced by oral elacridar and sunitinib coadministration. *Int J Cancer* 2012; **130**: 223–233.
24 Suzuki Y, Matsumoto Y, Ikeda Y, Kondo K, Ohashi N, Umemura K. SM-20220, a Na (+)/H(+) exchanger inhibitor: effects on ischemic brain damage through edema and neutrophil accumulation in a rat middle cerebral artery occlusion model. *Brain Res* 2002; **945**: 242–248.
25 Dwyer J, Le Guelte A, Galan Moya EM, Sumbal M, Carlotti A, Douguet L *et al.* Remodeling of VE-cadherin junctions by the human herpes virus 8 G-protein coupled receptor. *Oncogene* 2011; **30**: 190–200.
26 Cai XF, Jin X, Lee D, Yang YT, Lee K, Hong YS, Lee JH, Lee JJ. Phenanthroquinolizidine alkaloids from the roots of Boehmeria pannosa potently inhibit hypoxia-inducible factor-1 in AGS human gastric cancer cells. *J Nat Prod* 2006; **69**: 1095–1097.
27 Kung AL, Zabludoff SD, France DS, Freedman SJ, Tanner EA, Vieira A, Cornell-Kennon S, Lee J, Wang B, Wang J, Memmert K, Naegeli HU, Petersen F, Eck MJ, Bair KW, Wood AW, Livingston DM. Small molecule blockade of transcriptional coactivation of the hypoxia-inducible factor pathway. *Cancer Cell* 2004; **6**: 33–43.
28 Cattaneo MG, Cappellini E, Benfante R, Ragni M, Omodeo-Salè F, Nisoli E *et al.* Chronic deficiency of nitric oxide affects hypoxia inducible factor-1α (HIF-1α) stability and migration in human endothelial cells. *PLoS One* 2011; **6**: e29680.
29 Hashimoto A, Hashimoto S, Ando R, Noda K, Ogawa E, Kotani H *et al.* GEP100-Arf6-AMAP1-cortactin pathway frequently used in cancer invasion is activated by VEGFR2 to promote angiogenesis. *PLoS One* 2011; **6**: e23359.
30 Fukuhara S, Sakurai A, Sano H, Yamagishi A, Somekawa S, Takakura N *et al.* Cyclic AMP Potentiates vascular endothelial cadherin-mediated cell-cell contact to enhance endothelial barrier function through an Epac-Rap1 signaling pathway. *Mol Cell Biol* 2005; **25**: 136–146.
31 Connolly DT, Olander JV, Heuvelman D, Nelson R, Monsell R, Siegel N *et al.* Human vascular permeability factor. Isolation from U937 cells. *J Biol Chem* 1989; **264**: 20017–20024.
32 Clauss M, Gerlach M, Gerlach H, Brett J, Wang F, Familletti PC *et al.* Vascular permeability factor: a tumor-derived polypeptide that induces endothelial cell and monocyte procoagulant activity, and promotes monocyte migration. *J Exp Med* 1990; **172**: 1535–1545.

33 Lampugnani MG, Orsenigo F, Gagliani MC, Tacchetti C, Dejana E. Vascular endothelial cadherin controls VEGFR-2 internalization and signaling from intracellular compartments. *J Cell Biol* 2006; **174**: 593–604.
34 Lillis AP, Van Duyn LB, Murphy-Ullrich JE, Strickland DK. LDL receptor-related protein 1: unique tissue-specific functions revealed by selective gene knockout studies. *Physiol Rev* 2008; **88**: 887–918.
35 Lijnen HR, van Hoef B, Beelen V, Collen D. Characterization of the murine plasma fibrinolytic system. *Eur J Biochem* 1994; **224**: 863–871.
36 Suzuki Y, Nagai N, Collen D. Comparative effects of microplasmin and tissue-type plasminogen activator (tPA) on cerebral hemorrhage in a middle cerebral artery occlusion model in mice. *J Thromb Haemost* 2004; **2**: 1617–1621.
37 Garabedian HD, Gold HK, Leinbach RC, Yasuda T, Johns JA, Thornton D *et al.* Laboratory monitoring of hemostasis during thrombolytic therapy with recombinant human tissue-type plasminogen activator. *Thromb Res* 1988; **50**: 121–133.
38 Suzuki Y, Nagai N, Umemura K, Collen D, Lijnen HR. Stromelysin-1 (MMP-3) is critical for intracranial bleeding after t-PA treatment of stroke in mice. *J Thromb Haemost* 2007; **5**: 1732–1739.
39 Suzuki Y, Yasui H, Brzoska T, Mogami H, Urano T. Surface-retained tPA is essential for effective fibrinolysis on vascular endothelial cells. *Blood* 2011; **118**: 3182–3185.
40 Ben-Zvi A, Lacoste B, Kur E, Andreone BJ, Mayshar Y, Yan H *et al.* Mfsd2a is critical for the formation and function of the blood-brain barrier. *Nature* 2014; **509**: 507–511.

Supplementary Information accompanies the paper on the Journal of Cerebral Blood Flow & Metabolism website (http://www.nature.com/jcbfm)